The nature of hydrogen in x-ray photoelectron spectroscopy: General patterns from hydroxides to hydrogen bonding

S. J. Kerber
Material Interface, Inc., Sussex, Wisconsin 53089-2244

J. J. Bruckner
University of Wisconsin–Milwaukee, Milwaukee, Wisconsin 53201

K. Wozniak
University of Warsaw, Warsaw, Poland

S. Seal, S. Hardcastle, and T. L. Barr
University of Wisconsin–Milwaukee, Milwaukee, Wisconsin 53201

(Received 11 October 1995; accepted 25 March 1996)

Important progressive alterations in chemical bonding are often realized through correlations with shifts in the x-ray photoelectron spectroscopy (XPS) binding energies of key elements. For example, there are useful general XPS shifting schemes for such systems as oxides, nitrides, halides, and even various functional groups in organics. Very general patterns, based upon location in the periodic table, exist for many of these materials even when the structure is not strongly considered. Unfortunately, apparently because of the lack of direct XPS detection of hydrogen, there seems to be no general statements in the literature for describing hydrogen-containing compounds, despite the fact that synergistic shifts obviously exist in the XPS spectra of elements attached to hydrogen (e.g., for M–O–H vs M–O–M units, where M is a typical metal). While not attempting a complete review paper, in the present work we use XPS shifting patterns to evolve a series of interrelated covalency/ionicity arguments to help explain the progressive, periodic changes in XPS peak locations for such common cases as M–O–H- and M–N–H-containing systems. These arguments are followed by consideration of the less dramatic XPS shifting patterns exhibited by metal and metalloid hydrides, including organic bonding. The formalism concludes with a discussion of hydrogen bonding detected by XPS. After a select review of the infrequent use made by others to attribute XPS peak shifts to hydrogen bonding, we consider in some detail two cases recently published by members of our group. One case involves the formation of –N–H–N– bonds in proton sponge organic systems, while the other uses XPS to examine the formation of surface oriented –O–H–––O– bonds in the adsorption of peptides on oxidized metals. In the present article, the XPS patterns for these two seemingly divergent cases are explained by closely related arguments that may have far reaching generalities. © *1996 American Vacuum Society.*

I. INTRODUCTION

To inorganic chemists, hydrogen chemistry is recognized as one of the most regular and progressive features of the periodic table. Because of the abundance of hydrogen in our planetary system, this chemistry is one of the most prevalent in our experience. Further, hydrogen has a propensity to terminate the chemistry of many bonding environments, making it a natural feature of many surfaces. While x-ray photoelectron spectroscopy (XPS) is recognized as a preeminent tool for surface chemical analysis, a major shortcoming is that it cannot see hydrogen directly. Although the indirect XPS registration of the effects of hydrogen have been recognized for many years, the pros and cons of hydrogen analysis with XPS have not been collected and analyzed. It is our intent to use a number of specific examples to try to explain the general patterns of the XPS binding energies found in hydrogen chemistry.

The compounds containing hydrogen fall naturally into three classes: (a) the molecular hydrides, which include those systems containing –OH and –NH groups, (b) the salt-like hydrides of the alkali and alkaline earth metals, and (c) the interstitial hydrides of the transition metals. To this classification, we will follow Wells[1] and Pauling[2] and add a fourth group designated as that involving the hydrogen bond, i.e., X–H–Y, where X and Y are commonly either nitrogen or oxygen.

In this article we will begin with the molecular hydrides, which include ternary hydrides such as M–O–H and M–N–H. This discussion will be followed by a consideration of the metal and metalloid hydrides, including the vital class of carbon–hydrogen. The description culminates with what may be the most important case of all—hydrogen bonding, including our new evidence for the XPS detection of the presence of select hydrogen bonding, plus arguments for general patterns of hydrogen bonding and chemistry. In all of these cases the discussion will include a general interest in the bonding chemistry with particular concern on the XPS studies that have been accomplished for these systems.

For reasons of ultrahigh vacuum incompatibility, we will omit all cases in which the HM bond is extremely ionic,

either H^+ (e.g., HCl) or H^- (e.g., NaH). Similar restrictions prevent the measurements or XPS detection of the strong hydroxide bases (e.g., NaOH) and the strong oxyacids (e.g., H_2SO_4). However, certain features of these aggressively bonded materials may still be discerned from extrapolations of XPS data realized for more covalent systems.

II. MOLECULAR HYDRIDES

A. M–O–H and M–N–H bonds

A consideration of the chemical shifts realized by hydroxides can be arrived at by first examining the situation that results in the formation of oxides. Ignoring for a moment the influences of particular structures, one may consider a metal oxide to result in the creation of three-dimensional lattice structures containing M–O–M bonds. When this bonding forms, it has been traditional to classify the M–O bond as ionic. However, it should be apparent that even for the most reactive of metals (e.g., Rb), the M–O bond that is realized in oxide formation always has at least a small degree of covalency.[2,3] Thus it is more proper to consider the bonds realized in oxide formation to be mixed ionic/covalent bonds, even though they are generally dominated by the former. The interjection of a different M unit (M′, with a different electronegativity) to create M–O–M′, polarizes the bonding chemistry around the oxygen.[4,5] As the M–O bond becomes more covalent, the electrons become more diffuse, effectively moving away from the oxygen. In XPS, it has been shown that the position of the O 1*s* line in an oxide can be a measure of the relative covalency/ionicity of the oxide bond.[3,5]

In the specific case of M′ being hydrogen, i.e., the hydroxide cases, we will consider two features: first the changes in bonding chemistry as registered by XPS in going from M–O–M to M–O–H, and second, the XPS changes realized for the hydroxides when the M is varied. These features have been previously considered by Barr.[6] For the purposes of this discussion, M′–O–M′ will be considered to be H–O–H, or water. Little XPS work of solid water, i.e., ice, exists, but studies achieved thus far suggest a very large O 1*s* binding energy of approximately 533–534 eV.[3,7] This large value (relative to ionic oxides such as CaO with an O 1*s* of 529.9 eV) is consistent with the very covalent oxygen–hydrogen bond in neutral water. Based upon the arguments presented so far, one would anticipate that the interjection of the mixed M–O–H system will shift the O 1*s* from the water value of 534 down toward the values for the more ionic systems. In general, this means that the O 1*s* binding energy for hydroxide systems should occur between the O 1*s* value for the metal oxide and that for water. Data for experimental systems are included in Table I. Although it must be pointed out that this argument suffers from being exclusively initial states in form and ignoring final state shifts,[3,7,8] and although a few exceptions have been referenced in the literature,[9] this

TABLE I. Experimentally obtained XPS binding energies (in eV±0.1 eV) of select hydrogen-containing compounds and relevant nonhydrogen analogs. The data included are from variable sources which may have had dissimilar binding energy calibrations.

			H-containing compound		Non-hydrogen analog		
Element	Peak	B.E.	Compound	B.E.	Compound	B.E.	Ref.
O	1*s*		$Ni(OH)_2$	532.0	NiO	530.0	6
O	1*s*		$Cu(OH)_2$	531.7	CuO	530.3	6
O	1*s*		$Zr(OH)_4$	531.2	ZrO_2	529.9	6
Cu	$2p_{3/2}$	932.5	$Cu(OH)_2$	934.8	CuO	933.7	6
Pd	$3d_{5/2}$	335.4	$Pd(OH)_4$	338.6	PdO	336.9	6
Cd	$3d_{5/2}$	405.0	$Cd(OH)_2$	405.1	CdO	404.2	7
In	$3d_{5/2}$	444.0	$In(OH)_2$	445.8	In_2O_2	444.9	7
B	1*s*	186.5	$B_{10}H_{14}$	187.6			17
Ba	$3d_{5/2}$	780.6	BaH_2	782.0			7
Y	$3d_{5/2}$	155.8	YH_3	157.7			7
Zr	$3d_{5/2}$	178.8	ZrH_2	178.8			7
Nb	$3d_{5/2}$	202.2	NbH_2	202.9			16
Ti	$2p_{3/2}$	453.9	TiH_2	454.0			17
C	1*s*	284.6	C–O–H, alcohol	286.1	C–O–C, ether	285.7	13
O	1*s*		C–O–H, alcohol	532.8	C–O–C, ether	532.5	13
C	1*s*		O ‖ —C–OH	289.3	O ‖ —C*–OC O	289.0	13
C	1*s*		—C–N–H	285.7	‖ —C–NH	287.7	13,19
N	1*s*		NH_3	398.8	$C–NH_2$	399.5	7,13
P	2*p*	130.2	NaH_2PO_4	134.2	P_2O_5	135.2	3

method represents a generally successful formalism for the prediction of hydroxide bonding effects.

In forming the mixed oxide M–O–M′ system, the binding energies of both M and M′ are also generally altered. If M is more ionic than M′, then M is found to become even more ionic in the mixed system and the M cationlike unit has its binding energy increased.[3,5] Unfortunately, if M′ is hydrogen it cannot be directly detected, *we can only look at its effects on M and O.* Since most M's are most cationic toward O than H, the formation of a hydroxide should be registered in XPS by an increase in binding energy of both the O 1*s* and the M peaks.[3]

This argument holds true to varying degrees for all metals. As anticipated, the similarity in the ionicity of the transition metals yields similar O 1*s* binding energies for the different hydroxides (see Table I). For most transition metals M, the main oxide peak occurs at approximately 530 eV and the major hydroxide peak is shifted to a higher binding energy, usually by 1.2–2.3 V. As documented in the literature by Barr[3,6,10] and Brundle,[11] an outer hydroxide layer is present on the surface of native oxides of titanium, vanadium, copper, nickel, and others. One must be careful with absolute identifications, however, because this hydroxide peak can be coincidental with a lower intensity peak due to chemisorbed, polarized O_2, and at still higher binding energies, (~534 eV), an additional small peak is often present due to chemisorbed water and weakly adsorbed oxygen molecules.

Continuing to the right-hand side of the periodic table, one reaches the amphoteric oxides in groups III and IVA, e.g., aluminum and silicon. In these cases, the ionicity of any OH bonds that are formed is very similar to that exhibited by the oxide bonds, e.g., ~50% for Si. Thus, for example, the O 1*s* and Al 2*p* for α-alumina are 531 and 73.9 eV, respectively, whereas the same binding energies for gibbsite [$Al(OH)_3$] are 531.1 and 74.2 eV, respectively.[3,7] Similar behavior is exhibited by silica and its corresponding hydroxides. Such amphoteric behavior dissipates as one goes down the groups IIIA and IVA columns, with the oxides and hydroxides becoming more ''metallic'' in behavior, similar to those of the transition metals.[3,12]

For organics, similar considerations are possible for systems containing the C–O–H and C–O–C bonds. In a C–O–C containing (ether) system, the C 1*s* binding energy is about 285.6 eV and O 1*s* is about 532.5 eV. In the case of C–O–H alcohols, the carbon becomes somewhat more ionic and the C 1*s* peak therefore increases to about 286.1 eV. The O 1*s* also increases to approximately 532.8 eV (to reflect the covalency of the O–H bond).[13] Thus, carbon is a weak example of a metalloid. In organic acid systems, such as formic acid, these arguments do not necessarily apply because there is a C═O group that affects the covalent/ionic character of the balance of the –OH system in a more complicated fashion than the simple M–O–M′ arguments used above.[14]

As one goes further to the right-hand side and up in the periodic table, the bonding between M and O in a M_xO_y system becomes increasingly covalent. Eventually the large O 1*s* value rivals that of water and finally exceeds it. Therefore, the argument given above for metals is reversed. Unfortunately there are not significant amounts of data in the literature for these materials because of their ultrahigh vacuum incompatibility, e.g., alkali and alkaline earth hydroxides. However, data for phosphorus has been generated and organized previously by Barr[3] to demonstrate these arguments as included in Table I.

The M–N–H situation tends to be similar to, but less dramatic than, these M–O–H cases. Metal nitrides place nitrogen in an effectively −3 oxidation state, thus producing relatively low N 1*s* binding energies. The N 1*s* for CrN occurs at 396.8 eV and even the metalloid Si_3N_4 pushes the N 1*s* down to 397.7 eV.[7] It is anticipated that the N 1*s* binding energy for the corresponding metal amines will lie somewhere between that for the corresponding nitride and ammonia (398.8 eV).[7,15] The presence of the relatively covalent hydrogen/nitrogen bond in metal amines is predicted to drive the metal binding energy upwards. As one moves to the right-hand side in the periodic table the effects for nitrogen mirror those for oxygen but are less dramatic. Examples are presented in Table I for C–N systems. Very little information is available on P_xH_y systems, but one would expect that the trends would follow those for the NH system.

B. Metal hydrides

A number of previous publications report detectable chemical shifts for various metal hydrides, particularly the commercially important intermetallic alloys.[16] Much of these data are controversial due to the fact that some systems adsorb hydrogen instead of, or in addition to, chemically binding with it. In addition, the commonplace interaction between these metals and O_2 and/or H_2O substantially interferes with the hydride results. Further, many of the anhydrous hydrides of interest are corrosive to the steel of vacuum vessels and copper gaskets.

Table I demonstrates that XPS can generally distinguish between many elemental species and their corresponding hydrides, with the core peaks of the hydride generally exhibiting an increasing binding energy.[7,17] This is obviously due to the partial extraction of one electron from the metal by the hydrogen to create the hydride. With regard to the two sides of the periodic table, the shifts for hydrides on the left-hand side (metal) of the table often appear to be smaller than the shifts for the hydrides on the right-hand side (nonmetal) of the table. This may be due to the higher electronegativity of the nonmetallics. A word of caution is in order, however, since many of the reported XPS studies of nonmetal hydrides were conducted on gas phase samples rather than solids. Examples[7] include SiH_4 with a reported silicon binding energy of 107.1 eV relative to an elemental value of 99.7 eV, PH_3 with a phosphorus binding energy of 137.3 eV relative to elemental phosphorus at 130.2 eV, and H_2S with a sulfur value of 170.4 eV relative to elemental sulfur at 164.2 eV.[17] Gas phase systems do not have work functions (or Fermi edges), and if one were to assume values of about 5 eV for the former the reported large chemical shift for these hydride

materials essentially disappears. Establishing a proper Fermi edge (with appropriate treatment of charging) will reduce these differences even further.

C. Carbon–hydrogen systems

The involvement of hydrogen with carbonaceous systems has produced the largest number of chemical compounds in existence, however there is a relative similarity of the chemistries for many of these compounds. Thus, it is not surprising that XPS finds only marginal differences between the effects of C–H, C–C, and –C═C– bonds. As discussed earlier, the C–O–H bonding unit is relatively amphoteric and for this reason, the differences in XPS binding energies in going from M–O–M bonds to M–O–H that played a significant role in the previously described metal hydroxides are not as substantial in the case of carbon-based systems. Despite these qualifiers, certain examples of XPS differentiation have been found for carbonaceous systems with hydrogen.

For purposes of uniformity, the value of 284.6 eV is often selected as a point of reference for the hydrocarbon part of typical adventitious carbon, serving as a basis to describe all C_xH_y systems. However, several groups[18,19] have found that not all C_xH_y systems exhibit a singular binding energy, with values suggested to range from 285.3 eV (complex aliphatics) to 284.4 eV (graphite). For air exposed systems, one generally finds C 1*s* spectra with modest, but significant, shoulders on their high binding energy side due to the presence of CO_2, various carbonyl-containing organics in our environment, and substantial C–OH, a version of our previously considered M–OH units. The recently published book *High Resolution XPS of Organic Polymers* by Beamson and Briggs[13] has extensive binding energy tables that provide excellent registers of the peak positions and ranges for almost all of the common carbonaceous bond situations that are realizable, including those experiencing the effects of hydrogen. Using these tables, and our own data, we have found repetitive, generalized binding energies for C_xH_y and C–Z–H bonded systems where Z is typically O and N, as listed in Table I. The principal C_xH_y peak is assumed at 284.6 eV. Several types of C–O bonded systems can be identified, and as one can see in Table I, we suggest that with reasonable XPS resolution one can differentiate between C–O–C and C–O–H bonds. In addition, we find that there are noticeable binding energy positions where the C–N–H (~285.6 eV) and O═C–N–H (~287.7 eV) species are found.

III. HYDROGEN BONDING

A. General discussion

Hydrogen bonding, –X–H–X′–, is one of the least understood and most important concepts in chemical bonding. It is the basic reason for the unusual physical properties of water and for the three-dimensional double helical structure of DNA strands. The hydrogen bond forces certain structures to have particular crystalline behavior where often one might not expect crystallinity.[1,2] For example, the hydrogen bond constrains protein molecules to their native configurations. In the X–H–X′ model, X and X′ may be any species that is significantly electronegative, the most common cases being fluorine, oxygen, and nitrogen. Cases of mixed oxygen–hydrogen–nitrogen bonds are also common in biological systems.

Hydrogen forms a covalent bond with only one species, e.g., hydrocarbons or hydroxides.[1,2] Thus *hydrogen bonds*, in which hydrogen is bonded to two species, results in bonds that are neither totally covalent nor ionic. Pauling recognized that the hydrogen bond is primarily ionic in character.[2] Hydrogen bonds may be weak, with a bond energy perhaps as low as 2 kcal/mol. But recent studies have shown that particular forms, such as those discussed below, may have energies as large as 15 kcal/mol.[20] Because of the relatively small bond energy of the hydrogen bond and the small activation energy involved in its formation, the hydrogen bond often plays a part in near room temperature reactions. In the present circumstance, we will be considering two types of hydrogen bonds: (1) the bond formed between two nitrogen atoms in complex napthalenic organic crystals, and (2) the bond formed between two oxygen atoms during the absorption of peptides onto hydrated metal oxide surfaces.

B. Hydrogen bonding—DMAN

1,8 bis(dimethylamino)naphthalene (DMAN, Fig. 1) is the parent molecule of a class of compounds known as proton sponges.[21] The significant steric strain in DMAN is associated with the amine groups which are in close proximity. The strain may be relieved by sequestration of protons from mineral or organic acids, which lead to the formation of very stable ionic complexes containing hydrogen bonded $N–H–N^+$ bridges. As a consequence, proton sponges have enormous affinities for H^+ and thus strong basicities, typically $p\mathrm{Ka}=12$. Proton sponges are the analogs of certain superacids. Although some nuclear magnetic resonance (NMR) and other studies of hydrogen-bonded DMAN complexes have been published,[21] little is known about the parent molecule, especially in the solid state.[20] Recently, some members of our group have performed ^{13}C and ^{1}H magic angle spinning NMR spectroscopy[21,22] and XPS of DMAN[22,23] and its complexes.

A series of acid halide-substituted DMAN compounds were prepared by adding discrete amounts of various acid halides to DMAN powder in the liquid phase and then crystallizing the resultant complex to yield a structure that contains a hydrogen bond between the amino groups. The acid halides employed were HCl, HBr, and HI; all of these are classed as strong acids. In this study, XPS was used to determine if there were detectable differences that could be correlated to progressive features in hydrogen bonding.[22,23] For a substantial period of time, an XPS spectrum for DMAN itself was not obtained because it apparently sublimes at room temperature at approximately 10^{-3} Torr. Elaborate procedures were recently developed to circumvent this problem and implemented to permit detailed XPS analysis.

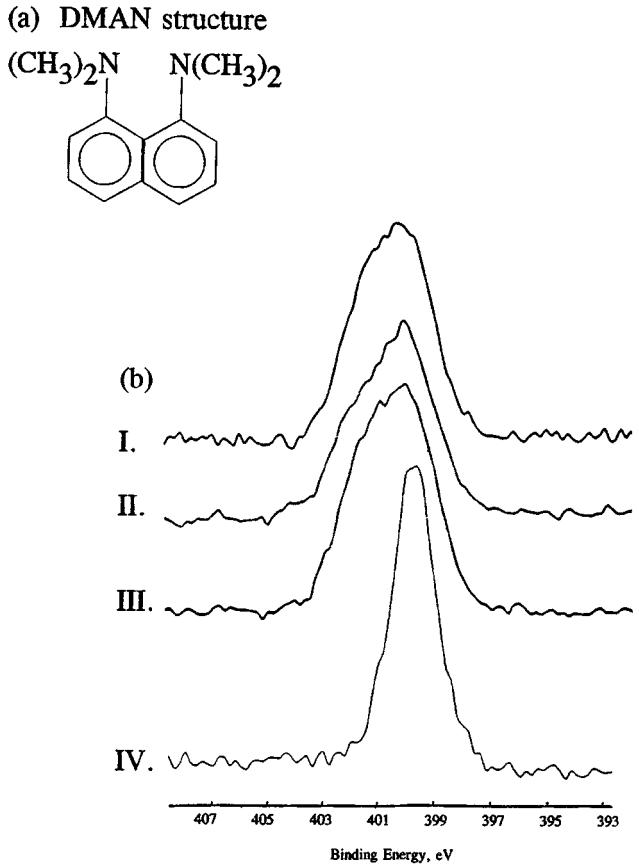

FIG. 1. (a) 1,8 bis(dimethylamino)naphthalene, DMAN and (b) XPS high resolution N 1*s* spectra of DMAN and its acid halide derivatives: I. HI, II. HBr, III. HCl, and IV. DMAN. The shift from DMAN to the left-hand side is speculated to be due to hydrogen bonding.

The carbon spectra (not illustrated) for DMAN are somewhat broadened and centered at about 285.0 eV suggesting a manifold of at least two peaks; one at ~284.6 eV (the hydrocarbon C 1*s*) and one at a higher energy, apparently indicative of the C–N bonds. Unreacted DMAN exhibits a narrow N 1*s* line at ~399.5 eV (no hydrogen bonding). The nitrogen spectra obtained for the acid halide derivatives, $DMANH^+X^-$ are illustrated in Fig. 1. The primary DMAN nitrogen at 399.5 eV is now spread into a clear multiplet, with the new peaks occurring 1–3 eV higher than the major peak. At times only a single secondary peak seems to occur whereas other cases exhibit an apparent manifold of peaks, perhaps as many as four.[22,23] Based on supporting XRD[22,23] and NMR[22,23] data and the direction of these XPS shifts we argue that the nature of the occurrence of these secondary peaks suggests their direct association with hydrogen bonding as a result of the acid substitution. The peaks seem to shift in position and relative size with changes in the halide series.

In addition to the hydrogen halides, hydrogen bonding in DMAN has been achieved with a number of other acids with similar results.[22,23] XPS of these systems provides spectra which in part repeat and vindicate the arguments used for the hydrogen halide (HX) substituted DMAN systems, i.e., positive H 1*s* shifts with H-bond formation. Features that are unique to the non-HX induced results include informative XPS peak patterns for the various anions. These anions include SCN^-, BF_4^-, CCl_3COO^-, ClO_4^-, and others. The results from those studies will be published at a later date.

The nitrogen from all of these types of hydrogen-shifted structures are expected to be shifted to a higher binding energy relative to the original nitrogen because there is the creation of a positive center, producing shifts similar to those detected between ammonia and ammonium ions (398.8 and 401.7 eV, respectively). Thus the upward shift reflects the formation of a quasication; the variances in that shift and peak size based upon acid type apparently reflect the variation in the strength of the hydrogen bond. Two of the N 1*s* peaks are indicative of the asymmetry previously ascribed to the proton position in the diamine H-bonding linkage.[21–23] Other features, such as the retention of unaltered DMAN and the prospect of variable proton positions are possible explanations for the multiplicity of these surface oriented XPS peaks. Further arguments are presented below on this subject.

C. Hydrogen bonding—peptide

A study regarding the adsorption of three peptides on two titanium alloys has been previously reported by Kerber.[24] The nature of the adhesion was found to be consistent with the formation of critical hydrogen bonds. The peptides were arginine–glycine–aspartic acid–serine (RGDS), arginine–glycine–aspartic acid–alanine (RGDA), and arginine–phenylalanine–aspartic acid–serine (RFDS). The titanium alloys were *cp*-Ti and Ti–6Al–4V. After an exposure to aqueous peptide solution for 26 h at 25 °C, the titanium samples were rinsed, dried, and analyzed with XPS. Adsorption isotherms were obtained for the six systems by plotting the adsorbed peptide N/Ti ratio over a concentration range of 0.0–0.2 mg/ml for the matrix of experiments. The shape of the isotherms supported the hypothesis that the peptides were bonded to the hydrated native titanium oxide surface via hydrogen bonding,[24] presumably between surface hydroxides and the peptide organic acid groups. Fourier transform infrared (FTIR) analysis gave strong indications that hydrogen bonding to the metallic surface had occurred.[25]

Typical titanium XPS spectra were obtained from both alloy surfaces, with 2*p* peaks occurring at 458.5 eV (titanium oxide) and at 453.8 eV (metallic titanium).[24] Because the TiO_2 signal was so strong, shoulder peaks from the expected surface oriented titanium hydroxides were found to be obscured by the stronger oxide peaks. There was no significant change in the titanium spectra with peptide adsorption. Peptide nitrogen was routinely detected at 400.9 eV; once again, there was no significant change in the nitrogen spectra with peptide adsorption.

The high resolution XPS O 1*s* spectra from RGDS powder, distilled-water exposed titanium, and titanium exposed to 2 mg/ml RGDS are shown in Fig. 2.[24] The primary oxygen peak for RGDS powder occurs at 531.2 eV, coinciding with C═O; a high energy tailing is also found, due apparently to

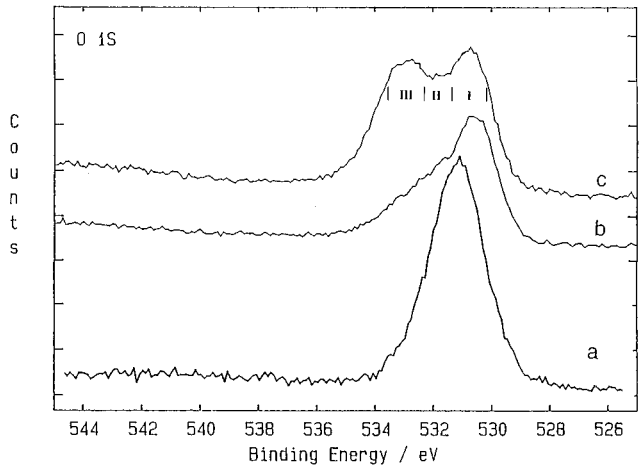

FIG. 2. XPS high resolution O 1*s* spectra from (a) RGDS powder, (b) Ti–6Al–4V exposed to distilled water, and (c) 2 mg/ml RGDS adsorbed from aqueous solution on Ti–6Al–4V. Region I corresponds to TiO_2 and C═O, region II to $Ti(OH)_4$, hydrated oxide, and C–OH, and region III to new features suggested to be due to Ti–O–H––O– C units between the hydrated titania surface and C–O bonds in RGDS.

C–OH oxygen at 532.5 eV. The O 1*s* spectra for the water-exposed titanium is primarily typical of the oxide portion of TiO_2 (530.7 eV) with high energy tailing, reflecting terminal hydroxide and aquation in a manner consistent with all air exposed oxides. After adsorption, in addition to undisturbed TiO_2, a series of peaks ranging from 531.5 to 533.5 eV increased (relative to the main oxygen peak at 530.7 eV) with increasing peptide solution concentration. The balance of the higher energy O 1*s* structure found in Fig. 2(c) was presumed to be due to the presence of, and chemical interaction between the peptide and the hydrated titania surface.[24]

In inspecting Fig. 2, it is apparent that some of the three distinct binding energy regions of spectra (c) can be associated with corresponding oxygen-containing parts of (a) and (b). Therefore, region I corresponds to the positions of TiO_2 and C═O, while the right-hand side of region II is close to $Ti(OH)_4$ and the left-hand side of region II is indicative of any hydrated metal oxide and C–OH. Region III, however, does not reflect any portion of (a) or (b). In view of the higher binding energy of region III and the lack of other candidates, the new feature is suggested to be due to Ti–O–H–––O–C units that may result from hydrogen bonding between the titania surface and RGDS. These features are clarified and the mechanisms for the attachment are described in Ref. 24.

D. XPS of hydrogen bonding—general remarks

We are not the first to employ XPS to help to describe hydrogen bonding. For example, Incorvia and Contarini[26] used XPS to investigate the adsorption of select, complex (inhibitor) amines on the surface of passivated iron. The system proves to be quite similar to our amine on Ti results. Thus, retention of the obvious metal–OH structure results with indication of the formation of Fe–O–H––N–R hydrogen bonds. The latter are shown to produce higher binding energy shifts in both the N 1*s* and O 1*s* peak manifolds and a corresponding (and quite interesting) lack of shift in the Fe (note the behavior of Ti in our studies). On the other hand, Nilsson *et al.*[27] employed XPS to follow the metal adsorption destruction of N–H–N-type hydrogen bonds. Similar XPS shifts to higher binding energy were detected by Bigelow *et al.*[28] in their XPS study of the production of intramolecular hydrogen bonding.

The general features of our XPS-hydrogen bonding studies are the introduction of H into a complex diamine system, DMAN, and the retention of hydroxides on air oxidized Ti to form –O–H–O bonds following adsorption of proteins. Both cases exhibit the same XPS patterns featuring positive shifts in the amino or hydrated units (–N–H–N– and –O–H–O–) and reduction in the positive shifts by the species attached to this unit (the carbons in one case and titanium and carbon in the other). In view of our previous discussion of the influence of the alterations in the bond covalency/ionicity on binding energy shifts, we turn to the conclusions of Pauling[2] and Wells,[1] who point out that the introduction of (–A–H–A–) hydrogen bonding produces a bond that is mixed of type, but primarily ionic. *This means that the balance of charge around the* A *unit requires that following hydrogen bonding the M–A bond must exhibit enhanced covalency.* As a result one should expect the binding energies of the A unit to increase and that for M to decrease. As started above, this is detected in both of our H bonding cases. The multiplicity of A≡N peaks in the acid substituted DMAN case primarily results from the asymmetry of the H^+ position between the two amine nitrogen. Thus, the C–N bond that is closest to the resulting proton is forced to be extremely covalent and its N 1*s* exhibits an increasing binding energy above 401 eV. The other C–N bond undergoes only a marginal increase in covalency, indicative of the N 1*s* at or below 400 eV.

IV. CONCLUSION

The present study concerns the influence of hydrogen in XPS. We have shown that although we are not able to detect hydrogen directly in this form of spectroscopy, one is usually able to detect and ascribe the effects induced by the presence of hydrogen into the XPS spectra of the elements that bond directly to it and even, in many cases, the elements (if any) that are bonded to the elements attached to hydrogen.

We have demonstrated these features by starting with a description of hydroxides and amines and showing how their XPS spectra differ from their corresponding oxides and nitrides. This discussion was followed by a cursory investigation of metal hydrides and how their XPS spectra differ from those of the elemental metals. The cases of organic C_xH_y, C–O–H, and C–N–H units were then considered as a unique collective set. The bonding for these systems obviously pivot on the unique properties of carbon and both its inherent amphoteric nature and unique propensity for covalent bonding. Both of these features play a central role in the relevance of carbon-based systems in hydrogen bonding—the final subject of our article.

In our study of H bonding we describe two quite divergent cases: one in which the H-bonding results from the substitution of H^+ ions into a basic system and the other in which there is evidence of H bonding following adsorption of peptides on a surface hydroxylated metal (Ti) oxide. Despite these obvious differences we have been able to show that the resulting XPS binding energy shifts induced by H bonding follow the same pattern, i.e., for M–A–H–A–M′ the binding energies of the A units are increased while those for M and M′ decrease. This, we explain, results from an enhancement of the covalency of the M–A bond induced by the creation of the relatively ionic A–H bonds. Evidence is also provided suggesting a substantial generality for these arguments.

[1]A. F. Wells, *Structural Inorganic Chemistry* (Clarendon, Oxford, 1945), Chap.7.
[2]L. Pauling, *The Nature of the Chemical Bond,* 3rd ed. (Cornell University Press, Ithaca, NY, 1960), Chaps. 3, 12.
[3]T. L. Barr, *Modern ESCA* (Chemical Rubber, Boca Raton, FL, 1994).
[4]J. A. Duffy, J. Phys. Chem. Glasses **30**, 1 (1989).
[5]T. L. Barr, J. Vac. Sci. Technol. A **9**, 1793 (1991).
[6]T. L. Barr, J. Phys. Chem. **82**, 1801 (1978).
[7]*Practical Surface Analysis,* 2nd ed., edited by D. Briggs and M. P. Seah (Wiley, Chichester, 1990).
[8]P. S. Bagus, C. R. Brundle, G. Pacchioni, and F. Parmigiani, Surf. Sci. Rep. **19**, 265 (1993).
[9]S. W. Gaarenstroom and N. Winograd, J. Chem. Phys. **67**, 3500 (1977).
[10]T. L. Barr, J. Vac. Sci. Technol. **14**, 650 (1977).
[11]C. R. Brundle, Faraday Discuss. Chem. Soc. **60**, 159 (1975).
[12]F. A. Cotton and G. Wilkinson, *Advances in Inorganic Chemistry,* 5th ed. (Wiley, New York, 1988).
[13]G. Beamson and D. Briggs, *High Resolution XPS of Organic Polymers* (Wiley, Chichester, 1992).
[14]T. L. Barr and M. P. Yin, J. Vac. Sci. Technol. A **10**, 2788 (1992).
[15]F. P. Larkins and A. Lubenfeld, J. Electron Spectrosc. Relat. Phenom. **15**, 137 (1979).
[16]K. Tanaka, M. Ushida, K. Sumiyama, and Y. Nakamura, J. Non-Cryst. Solids **117-118**, 429 (1990); K. Tanaka and H. Aoki, J. Nucl. Mater. **169**, 299 (1989).
[17]C. D. Wagner, W. M. Riggs, L. E. Davis, J. F. Moulder, and G. E. Muilenberg, *Handbook of X-Ray Photoelectron Spectroscopy* (Perkin–Elmer, Eden Prairie, MN, 1979).
[18]G. Barth, R. Linder, and C. Bryson, Surf. Interface Anal. **11**, 307 (1988).
[19]T. L. Barr, S. Seal, S. Krezoski, and D. H. Petering, Surf. Interface Anal. (in press).
[20]A. Warohel, A. Papazyan, and P. A. Kollman, Science **269**, 102 (1995); W. W. Cleland and M. M. Kreevoy, *ibid.* **269**, 104 (1995); P. A. Frey, *ibid.* **269**, 104 (1995).
[21]K. Wozniak, H. He, J. Klinowski, and E. Grech, J. Phys. Chem. **99**, 1403 (1995).
[22]K. Wozniak, H. He, J. Klinowski, W. Jones, and T. L. Barr, J. Phys. Chem. **99**, 14667 (1995).
[23]K. Wozniak, H. He, J. Klinowski, W. Jones, T. L. Barr, and S. Hardcastle, J. Phys. Chem. (in press).
[24]S. J. Kerber, J. Vac. Sci. Technol. A **13**, 2619 (1995).
[25]S. J. Kerber, H. Mueller, and T. L. Barr (unpublished).
[26]M. J. Incorvia and S. Contarini, J. Electrochem. Soc. **136**, 2493 (1989).
[27]J. O. Nilsson, C. Tornkvist, and B. Liedberg, Appl. Surf. Sci. **37**, 306 (1989).
[28]R. W. Bigelow, K. Y. Law, P. H. K. Pan, and H. J. Freund, J. Electron Spectrosc. Relat. Phenom. **46**, 1 (1988).